

η' meson production in proton-proton collisions

K. Nakayama^{a,b}, H. F. Arellano^c, J. W. Durso^{a,d}, and J. Speth^a

^a*Institut für Kernphysik, Forschungszentrum-Jülich, D-52425, Jülich, Germany*

^b*Department of Physics and Astronomy, University of Georgia, Athens, GA 30602, USA*

^c*Departamento de Física, Facultad de Ciencias Físicas y Matemáticas, Universidad de Chile,*

Blanco Encalada 2008, Santiago, Chile

^d*Physics Department, Mount Holyoke College, South Hadley, MA 01075, USA*

Abstract

The $pp \rightarrow pp\eta'$ reaction is investigated within a relativistic meson-exchange model of hadronic interactions. We explore the role of nucleonic and mesonic, as well as the N^* resonance currents, in producing η' mesons. In order to learn more about the production mechanisms, new measurements in the energy region far from the threshold are required.

PACS: 13.60Le, 25.10+s, 25.40-h

I. INTRODUCTION

With the advent of particle accelerators in the few GeV energy region, heavy meson production in hadronic collisions has attracted increasing attention in the past few years. In particular, heavy meson production in nucleon-nucleon (NN) collisions at near-threshold energies is of special interest, not only because it is suited for extracting information on a few lowest-order multipole amplitudes, but also because it is considered to provide important information on the short distance behavior of the NN interaction. Due to the large momentum transfer between the initial and final nucleons, these reactions at near-threshold energies necessarily probe the NN interaction at short distances. In the present work we concentrate on the η' meson production in proton-proton (pp) collisions.

Among heavy mesons, the η' meson is of particular interest for various reasons. The η' meson is thought to couple strongly to gluons via the QCD anomaly coupling $\eta' \rightarrow g + g$ [1]. Also, an unexpectedly large branching ratio measured recently for the inclusive decay of beauty particles, $B \rightarrow \eta' + X$ [2] has been interpreted as possible evidence for the strong coupling of η' meson to the gluonic components [3]. It would then be conceivable that the $pp \rightarrow pp\eta'$ reaction might probe the gluon content of the η' meson via its coupling to gluons emitted from the quarks exchanged between two interacting nucleons. This mechanism would be complementary to the vector meson-exchange current mechanism for producing η' mesons.

One of the properties of the η' meson of extreme importance is its yet-poorly-known coupling strength to the nucleon. This has attracted much attention in connection with the so-called "nucleon-spin crisis" in polarized deep inelastic lepton scattering [4]. The $NN\eta'$ coupling constant, $g_{NN\eta'}$, may be related (through the axial vector coupling using the Goldberger-Treiman relation) to the quark helicity contribution to the spin of the proton [5]. Therefore one can argue that $g_{NN\eta'}$ tells us about the total spin of the nucleon carried by its constituents; conversely, the quark contribution to the spin of the nucleon would tell us about $g_{NN\eta'}$. So far there is no direct experimental measurement of $g_{NN\eta'}$. Recently, cross

sections for the $pp \rightarrow pp\eta'$ reaction near threshold have been measured by the COSY-11 [6] and SPESIII [7] collaborations. This reaction may offer an opportunity to determine this coupling from a direct emission process of η' by a proton. Of course, other production mechanisms, such as meson exchange and nucleon resonance currents, must be taken into account before a quantitative determination of $g_{NN\eta'}$ is possible. The major aim of the present work is to explore the roles of various production mechanisms.

The theory of η' production in pp collisions is still in its early stage of development [8–11]. In this work we investigate this reaction using a relativistic meson-exchange model of hadronic interactions. In section 2 we outline the formalism for calculating the production amplitude. The final state interaction is known to play a crucial role in the production of particles near threshold energies in NN collisions [12]; therefore our formalism includes the pp final state interaction explicitly. The Coulomb correction in the pp final state interaction is also known to be important when these protons have small energies [13,14]. In the present work it is treated exactly and reduces the calculated cross section by as much as a factor of two for energies close to threshold. The initial state interaction is taken into account via a reduction factor [15] determined from the available phase shifts and inelasticities in the threshold incident energy region. In section 3 our η' meson production currents are constructed. We consider the nucleonic, mesonic and resonance currents. The roles of these currents are explored in section 4. Our results are summarized in Section 5.

II. FORMALISM

The formalism used in the present work is essentially the same as that employed in Refs. [17,18] for studying the production of vector mesons. It is based on a relativistic meson-exchange model of hadronic interactions in which the transition amplitude is calculated in the Distorted Wave Born Approximation, taking explicitly into account effects of the final state interaction. We write the transition amplitude describing the $p+p \rightarrow p+p+\eta'$ process as

$$M = \langle \phi_f | (T_f^{(-)\dagger} iG_f + 1) J | \phi_i \rangle , \quad (1)$$

where $\phi_{i,f}$ denotes the four-component unperturbed pp wave function in the initial (i) and final (f) state. $T_f^{(-)}$ is the final state pp T-matrix. G_f stands for the two-nucleon propagator and J is the η' -emission current defined in the next section.

The T-matrix used in our calculation is generated by solving a three-dimensional reduced Bethe-Salpeter equation (the Blankenbecler-Sugar equation) for a relativistic one-boson-exchange NN potential V , i.e.,

$$T = V + ViG_{BBS}T , \quad (2)$$

where G_{BBS} denotes the Blankenbecler-Sugar (BBS) two-nucleon propagator. In this work we employ a slightly modified version [19] of the Bonn B NN model as defined in Table A.1 of Ref. [20] for constructing the potential V . This modification has been made in order to reproduce the pp low-energy parameters rather than the pn low-energy parameters while preserving other features of the Bonn B interaction model for describing pp scattering [19]. It should also be mentioned that each nucleon-nucleon-meson (NNM) vertex in the NN potential is modified by a form factor of either monopole or dipole form. We refer to [20] for further details. Furthermore we note that the two-nucleon propagator G_f appearing in Eq.(1) is, for consistency, also chosen to be the BBS propagator, $G_f = G_{f;BBS}$.

In Eq.(1) the initial state interaction is neglected. For heavy meson production such as η' , its effect on the production cross sections near threshold may be taken into account by multiplying the calculated cross sections using Eq.(1) by a factor [15]

$$\lambda_\alpha = \eta_\alpha \cos^2(\delta_\alpha) + \frac{1}{4}[1 - \eta_\alpha]^2 \quad (3)$$

where α stands for the quantum numbers specifying the corresponding initial NN state and δ_α and η_α denote the corresponding NN phase-shift and inelasticity, respectively, at the nucleon incident energy. Although this reduction factor is only meant to account for the gross effect of the initial state interaction, it works well when confronted with a calculation where the initial state interaction has been treated explicitly [21]. In the near threshold

energy region the relevant initial pp state is $\alpha = {}^3P_0$. For η' production the threshold incident energy is about $T_{lab} = 2.404 \text{ GeV}$. Using the values $\delta_{{}^3P_0} = -50^\circ$ and $\eta_{{}^3P_0} = 0.75$ from a partial wave analysis [22], we obtain the reduction factor of $\lambda_\alpha = 0.33$ for the cross section. An alternative way to account for effects of the initial state interaction is to absorb these effects in the form factors at the η' meson production vertices as has been done in Refs. [17,18]. We choose the former method in the present work.

III. PRODUCTION CURRENTS

Within our hadronic model of strong interactions, the η' -emission current J in Eq.(1) consists of a sum of the baryonic and mesonic currents. The baryonic current is further divided into the nucleonic and nucleon resonance (N^*) currents, so that the total current is given by

$$J = J_{nuc} + J_{res} + J_{mec} . \quad (4)$$

The individual currents are illustrated diagrammatically in Fig. 1. In the following subsections we construct each of these currents.

A. The Nucleonic Current

The nucleonic current is defined as

$$J_{nuc} = \sum_{j=1,2} (\Gamma_j i S_j U + U i S_j \Gamma_j) , \quad (5)$$

with Γ_j denoting the $NN\eta'$ vertex and S_j the nucleon (Feynman) propagator for nucleon j . The summation runs over the two interacting nucleons, 1 and 2. U stands for the meson-exchange NN potential. It is, in principle, identical to the potential V appearing in the NN scattering equation, except that here meson retardation effects (which are neglected in the potential entering in Eq.(2)) are kept as given by the Feynman prescription.

The structure of the $NN\eta'$ vertex, Γ_j , in Eq.(5) is derived from the Lagrangian density

$$\mathcal{L}(x) = -g_{NN\eta'} \bar{\Psi}_N(x) \gamma_5 \left[\left(i\lambda + \frac{1-\lambda}{2m_N} \gamma^\mu \partial_\mu \right) \eta'(x) \right] \Psi_N(x) , \quad (6)$$

where $g_{NN\eta'}$ denotes the $NN\eta'$ coupling constant and λ is the parameter controlling the pseudoscalar(ps) - pseudovector(pv) admixture. $\eta'(x)$ and $\Psi_N(x)$ stand for the η' and nucleon field, respectively; m_N denotes the nucleon mass.

As mentioned in the introduction, the coupling constants $g_{NN\eta'}$ and the ps-pv mixing parameter λ are poorly known at present. The predictions for $g_{NN\eta'}$ range anywhere from 1.9 to 7.5 [23,24,9]; an estimate based on the dispersion method even gives $g_{NN\eta'}$ consistent with zero [25]. Zhang et al. [24] in their analysis of the photoproduction on protons of η' mesons used $\lambda = 1$ for the ps-pv mixing parameter. Bernard et al. [9], in their analysis of the $pp \rightarrow pp\eta'$ process, extracted a value of $\lambda = 0.4 \pm 0.1$ in conjunction with the value of $g_{NN\eta'} = 2.5 \pm 0.7$ determined from a recent measurements of $\Delta\Sigma$ in deep inelastic lepton-nucleon scattering [26]. The latter quantity is related to $g_{NN\eta'}$ [5]. SU(3) symmetry, together with the OZI rule [27], relates the $NN\eta'$ coupling to the $NN\eta$ coupling: $g_{NN\eta'} = g_{NN\eta} \tan(\alpha_P)$, where $\alpha_P \equiv \theta_P - \theta_{P(ideal)} \simeq -45^\circ$ denotes the deviation from the pseudoscalar ideal mixing angle. With the value of $g_{NN\eta} = 6.14$ used in NN scattering analysis [20], we then have $g_{NN\eta'} \simeq 6.1$ which is close to the upper end of the predicted range mentioned above. The value of $g_{NN\eta} = 6.14$ together with the $\eta - \eta'$ mixing angle of $\theta_P \simeq -9.7^\circ$, as suggested by the quadratic mass formula, and the $NN\pi$ coupling constant of $g_{NN\pi} = 13.45$ leads to the ratio $D/F \simeq 1.43$. This is not too far from the value of $D/F \cong 1.73$ extracted from a systematic analysis of semileptonic hyperon decays [28]. In the present work we use the value of $g_{NN\eta'} = 6.1$. We shall consider both of the extreme values of the parameter λ in Eq.(6), i.e., $\lambda = 0$ and 1. Note that η' is *not* a Goldstone boson. Consequently there is, *a priori*, no constraint on the ps-pv admixture.

The $NN\eta'$ vertex derived from Eq.(6) should be provided with an off-shell form factor. Following Ref. [18], it is assumed to be of the form

$$F_N(l^2) = \frac{\Lambda_N^4}{\Lambda_N^4 + (l^2 - m_N^2)^2} , \quad (7)$$

where l^2 denotes the four-momentum squared of either the incoming or outgoing off-shell nucleon. We also introduce the form factor given by Eq.(7) at those NNM vertices appearing next to the η' -production vertex, where the (intermediate) nucleon and the exchanged mesons are off their mass shell (see Fig. 1). Therefore, the corresponding form factors are given by the product $F_N(l^2)F_M(q_M^2)$, where M stands for each of the exchanged mesons between the two interacting nucleons. The form factor $F_M(q_M^2)$ accounts for the off-shellness of the exchanged meson and is taken consistently with the NN potential used for generating the T-matrix. In Ref. [18] cutoff parameters in the range of $\Lambda_N = 1.17 - 1.55 \text{ GeV}$ have been used in the description of ϕ - and ω -meson productions in pp collisions. In order to reduce the number of free parameters, here, we adopt the value of $\Lambda_N = 1.2 \text{ GeV}$, which is also the value adopted at the $NN^*\eta'$ vertex in the construction of the resonance current in the next subsection.

B. The Resonance Current

Currently there are no well established nucleon resonances that decay into $N\eta'$. In Ref. [24] the strong peak in the total cross section of the η' photoproduction off protons close to threshold has been attributed to the $D_{13}(2080)$ resonance. On the other hand, a recent multipole analysis of the η' photoproduction [16] indicates that this reaction is dominated by an S_{11} and a P_{11} resonance. In Ref. [16], apart from the resonance dominance assumption—which probably leads to an overestimation of the total decay width of the resonances considered, it is also assumed that these resonances decay only into $p\eta'$ and $p\pi^0$. The latter decay channel also effectively accounts for all other decay channels that were not considered explicitly in the analysis due to lack of information. Although this may not affect appreciably the description of the η' photoproduction reaction, the $pp \rightarrow pp\eta'$ process can be very sensitive to such an assumption. Since the pion couples strongly to the nucleon, an overestimation of the $p\pi^0$ partial decay width is likely to lead to a considerable overestimation of the cross section due to these resonances in the $pp \rightarrow pp\eta'$ reaction. In

addition to all these uncertainties in the extraction of the resonance parameters, there is also the possibility of a threshold cusp effect, as discussed in Ref. [29], that might explain the observed behavior of the photoproduction cross section close to threshold in the absence of any resonance. All these issues require further careful considerations. With this background in mind we will explore the role of the $S_{11}(1897)$ and $P_{11}(1986)$ resonances as determined in Ref. [16].

The resonance current, in analogy to the nucleonic current, is written as

$$J_{res} = \sum_{j=1,2} \sum_{N^*} \left(\Gamma_{jN^*\eta'} i S_{N^*} U_{N^*} + \tilde{U}_{N^*} i S_{N^*} \Gamma_{jN^*\eta'} \right) . \quad (8)$$

Here $\Gamma_{jN^*\eta'}$ stands for the $NN^*\eta'$ vertex function involving the nucleon j . $S_{N^*}(p) = (\not{p} + m_{N^*})/(p^2 - m_{N^*}^2 + im_{N^*}\Gamma_{N^*})$ is the N^* resonance propagator, with m_{N^*} and Γ_{N^*} denoting the mass and width of the resonance, respectively. The summation runs over the two interacting nucleons, $j = 1$ and 2 , and also over the resonances considered, i.e., $N^* = S_{11}(1897)$, $P_{11}(1986)$. In the above equation U_{N^*} (\tilde{U}_{N^*}) stands for the $NN \rightarrow NN^*$ ($NN^* \rightarrow NN$) meson-exchange transition potential. It is given by

$$U_{N^*} = \Gamma_{NN^*\pi}(q_\pi) i \Delta_\pi(q_\pi^2) \Gamma_{NN\pi}(q_\pi) , \quad (9)$$

where $\Delta_\pi(q_\pi^2)$ denotes the (Feynman) propagator of the exchanged pion with four-momentum q_π and $\Gamma_{NN\pi}(q_\pi)$ the $NN\pi$ vertex. The latter is taken consistently with the NN potential V appearing in Eq.(2). We note that there is also an additional contribution to U_{N^*} from the η' exchange in Eq.(9). However this is negligible compared to the pion-exchange contribution.

Following Ref. [30], the $NN^*\eta'$ and $NN^*\pi$ vertices in Eqs.(8,9) are obtained from the interaction Lagrangian densities

$$\begin{aligned} \mathcal{L}_{NN^*\eta'}^{(\pm)}(x) &= -g_{NN^*\eta'} \bar{\Psi}_N(x) \left\{ \left[i\lambda\Gamma^{(\pm)} + \left(\frac{1-\lambda}{m_{N^*} \pm m_N} \right) \Gamma_\mu^{(\pm)} \partial^\mu \right] \eta'(x) \right\} \Psi_{N^*}(x) + h.c. \\ \mathcal{L}_{NN^*\pi}^{(\pm)}(x) &= -g_{NN^*\pi} \bar{\Psi}_N(x) \left\{ \left[i\lambda\Gamma^{(\pm)} + \left(\frac{1-\lambda}{m_{N^*} \pm m_N} \right) \Gamma_\mu^{(\pm)} \partial^\mu \right] \vec{\tau} \cdot \vec{\pi}(x) \right\} \Psi_{N^*}(x) + h.c. , \end{aligned} \quad (10)$$

where $\vec{\pi}(x)$ and $\Psi_{N^*}(x)$ denote the pion and nucleon resonance field, respectively. The upper and lower signs refer to the even(+) and odd(-) parity resonance, respectively. The operators $\Gamma^{(\pm)}$ and $\Gamma_\mu^{(\pm)}$ in the above equation are given by

$$\begin{aligned}
\Gamma^{(+)} &= \gamma_5, \Gamma_\mu^{(+)} = \gamma_\mu \gamma_5 \\
\Gamma^{(-)} &= 1, \Gamma_\mu^{(-)} = \gamma_\mu.
\end{aligned} \tag{11}$$

The parameter λ in Eq.(10) controls the admixture of the two types of couplings: ps ($\lambda = 1$) and pv ($\lambda = 0$) in the case of an even parity resonance and, scalar ($\lambda = 1$) and vector ($\lambda = 0$) in the case of an odd parity resonance. On-shell, both choices of the parameter λ are equivalent. Hereafter the mixing parameter λ for the $NN^*\pi$ vertex is fixed to be $\lambda = 0$. We consider the choices $\lambda = 0$ and 1 in the $NN^*\eta'$ vertex, however.

The coupling constants $g_{NN^*\eta'}$ and $g_{NN^*\pi}$ are determined from the extracted decay widths (and masses) of the resonances from the η' photoproduction on protons [16],

$$\begin{aligned}
(m_{S_{11}}, \Gamma_{S_{11}}) &= (1.897 \pm 0.050_{-0.002}^{+0.030}, 0.396 \pm 0.155_{-0.045}^{+0.035}) \text{ GeV} \\
(m_{P_{11}}, \Gamma_{P_{11}}) &= (1.986 \pm 0.026_{-0.030}^{+0.010}, 0.296 \pm 0.100_{-0.010}^{+0.060}) \text{ GeV},
\end{aligned} \tag{12}$$

with partial decay widths

$$\begin{aligned}
\Gamma(S_{11} \rightarrow p\eta') &= 0.05\Gamma_{S_{11}}, \Gamma(S_{11} \rightarrow p\pi^0) = 0.95\Gamma_{S_{11}} \\
\Gamma(P_{11} \rightarrow p\eta') &= 0.25\Gamma_{P_{11}}, \Gamma(P_{11} \rightarrow p\pi^0) = 0.75\Gamma_{P_{11}}.
\end{aligned} \tag{13}$$

Using these values we obtain

$$\begin{aligned}
g_{NS_{11}\eta'} &= 2.9, g_{NS_{11}\pi} = 2.4 \\
g_{NP_{11}\eta'} &= 11.7, g_{NP_{11}\pi} = 5.2.
\end{aligned} \tag{14}$$

Here we assume the coupling constants to be positive. We mention in advance that the interference of the resonance current with the rest of the currents (nucleonic and mesonic currents) is practically negligible.

In complete analogy to the nucleonic current, we introduce the off-shell form factors at each vertex involved in the resonance current. We adopt the same form factor given by Eq.(7), with m_N replaced by m_{N^*} at the $NN^*\eta'$ and $NN^*\pi$ vertices, in order to account for the off-shellness of the N^* resonances. We note that Zhang et al. [24] have also employed

this form for the form factor at the $NN^*\eta'$ vertex in their study of η' photoproduction. In order to account for the off-shellness of the exchanged pion (see Eq.(9)), the $NN^*\pi$ vertex is also multiplied by an extra form factor of $F_\pi(q_\pi^2) = (\Lambda_\pi^2 - m_\pi^2)/(\Lambda_\pi^2 - q_\pi^2)$, the same form used at the $NN\pi$ vertex in the construction of the NN potential V entering in Eq.(2), with the cutoff parameter of $\Lambda_\pi = 0.8 \text{ GeV}$. We also use the same form factor at the $NN\pi$ vertex in Eq.(9).

C. The Mesonic Current

For the meson-exchange current we consider the contribution from the $vv\eta'$ vertex with v denoting either a ρ or ω meson. As we shall show later, this gives rise to the dominant meson-exchange current. The $vv\eta'$ vertex required for constructing the meson-exchange current is derived from the Lagrangian densities

$$\begin{aligned}\mathcal{L}_{\rho\rho\eta'}(x) &= -\frac{g_{\rho\rho\eta'}}{2m_\rho}\varepsilon_{\alpha\beta\nu\mu}\partial^\alpha\vec{\rho}^\beta(x)\cdot\partial^\nu\vec{\rho}^\mu(x)\eta'(x) \\ \mathcal{L}_{\omega\omega\eta'}(x) &= -\frac{g_{\omega\omega\eta'}}{2m_\omega}\varepsilon_{\alpha\beta\nu\mu}\partial^\alpha\omega^\beta(x)\partial^\nu\omega^\mu(x)\eta'(x) ,\end{aligned}\tag{15}$$

where $\varepsilon_{\alpha\beta\nu\mu}$ is the Levi-Civita antisymmetric tensor with $\varepsilon_{0123} = +1$. The vector meson-exchange current is then given by

$$J_{vv\eta'} = \sum_{v=\rho,\omega} \left\{ [\Gamma_{NNv}^\alpha(k_v)]_1 iD_{\alpha\beta}(k_v) \Gamma_{vv\eta'}^{\beta\mu}(k_v, k'_v) iD_{\mu\nu}(k'_v) [\Gamma_{NNv}^\nu(k'_v)]_2 \right\} ,\tag{16}$$

where $D_{\alpha\beta}(k_v)$ and $D_{\mu\nu}(k'_v)$ stand for the (Feynman) propagators of the two exchanged vector mesons (either the ρ or ω mesons as $v = \rho$ or ω) with four-momentum k_v and k'_v , respectively. The vertices Γ involved in the above equation are self-explanatory. The NNv vertex $\Gamma_{NNv}^\mu(v = \rho, \omega)$ is taken consistently with those in the potential used for constructing the NN T-matrix in Eq.(2).

The coupling constant $g_{vv\eta'}$ is determined from a systematic analysis of the radiative decay of pseudoscalar and vector mesons in conjunction with vector-meson dominance. This is done following Refs. [31,18], with the aid of an effective Lagrangian with SU(3) flavor

symmetry and imposition of the OZI rule. The parameters of this model are the angle $\alpha_V(\alpha_P)$, which measures the deviation from the vector(pseudoscalar) ideal mixing angle, and the coupling constant of the effective SU(3) Lagrangian. They are determined from a fit to radiative decay of pseudoscalar and vector mesons. The parameter values determined in this way in Ref. [31] (model B), however, overpredict the measured radiative decay width of the η' meson [32]. Therefore, we have readjusted slightly the value of the coupling constant of the SU(3) Lagrangian in order to reproduce better the measured width. We have $\alpha_V \cong 3.8^\circ$ and $\alpha_P \cong -45^\circ$, as given by the quadratic mass formula, and the coupling constant of the effective SU(3) Lagrangian of $G = 7$ in units of $1/\sqrt{m_v m'_v}$, where m_v and m'_v stand for the mass of the two vector-mesons involved. The sign of the coupling constant G is consistent with the sign of the $\rho\pi\gamma$ and $\omega\pi\gamma$ coupling constants taken from an analysis of the pion photoproduction data in the ~ 1 GeV energy region [33]. With these parameter values we obtain

$$\begin{aligned} g_{\rho\rho\eta'} &= -G \sin(\alpha_P) = 4.95 \\ g_{\omega\omega\eta'} &= -G \left(\sqrt{2} \sin^2(\alpha_V) \cos(\alpha_P) + \cos^2(\alpha_V) \sin(\alpha_P) \right) = 4.90 . \end{aligned} \quad (17)$$

The $vv\eta'$ vertex ($v = \rho, \omega$) in Eq.(16), where the exchanged vector mesons are both off their mass shells, is accompanied by a form factor. Following Ref. [18], we assume the form

$$F_{vv\eta'}(k_v^2, k_v'^2) = \left(\frac{\Lambda_v^2 - m_v^2}{\Lambda_v^2 - k_v^2} \right) \left(\frac{\Lambda_v^2}{\Lambda_v^2 - k_v'^2} \right) . \quad (18)$$

It is normalized to unity at $k_v^2 = m_v^2$ and $k_v'^2 = 0$, consistent with the kinematics at which the value of the coupling constant $g_{vv\eta'}$ was determined. We adopt the cutoff parameter value of $\Lambda_v = 1.45$ GeV as determined in Ref. [18] from the study of the ω and ϕ meson production in pp collisions.

Another potential candidate for mesonic current is the $\sigma\eta\eta'$ -exchange current, whose coupling constant may be estimated from the decay width of η' into an η and two pions. We take the Lagrangian densities

$$\mathcal{L}_{\sigma\eta\eta'}(x) = \frac{g_{\sigma\eta\eta'}}{\sqrt{m_\eta m_{\eta'}}} \sigma(x) \partial_\mu \eta(x) \partial^\mu \eta'(x)$$

$$\mathcal{L}_{\sigma\pi\pi}(x) = \frac{g_{\sigma\pi\pi}}{2m_\pi} \sigma(x) \partial_\mu \vec{\pi}(x) \cdot \partial^\mu \vec{\pi}(x) , \quad (19)$$

where $\sigma(x)$ and $\eta(x)$ stand for the σ and η meson field, respectively, and m_π , m_η and $m_{\eta'}$ stand for the masses of the π , η and η' meson. With the coupling constant of $g_{\sigma\pi\pi} \sim 1.3$, extracted from Ref. [34] in conjunction with the $NN\sigma$ coupling constant used in the NN potential V , and assuming that the measured decay width of $\Gamma(\eta' \rightarrow \eta + 2\pi^0) = 42 \text{KeV}$ [32] is entirely due to the σ meson intermediate state, we obtain an (upper) estimate of $|g_{\sigma\eta\eta'}| \sim 1.14$. The sign of this coupling constant is not fixed. We shall consider both possibilities.

The $\sigma\eta\eta'$ current reads

$$J_{\sigma\eta\eta'} = \left\{ [\Gamma_{NN\sigma}]_1 i\Delta_\sigma(q_\sigma^2) \Gamma_{\sigma\eta\eta'}(q_\sigma, q_\eta) i\Delta_\eta(q_\eta^2) [\Gamma_{NN\eta}(q_\eta)]_2 \right\} + (1 \leftrightarrow 2) \quad (20)$$

in our previously-defined notation. The vertices $\Gamma_{NN\sigma}$ and $\Gamma_{NN\eta}$ are taken consistently with those in the NN potential V in Eq.(2). The $\sigma\eta\eta'$ vertex, $\Gamma_{\sigma\eta\eta'}(q_\sigma, q_\eta)$, is provided with the same form factor given by Eq.(18), except for the replacement $m_v \rightarrow m_\eta$.

The total mesonic current is then given by

$$J_{mec} = J_{vv\eta'} + J_{\sigma\eta\eta'} . \quad (21)$$

There are, of course, other possible mesonic currents, such as the $\omega\phi\eta'$ - and $\phi\phi\eta'$ -exchange currents, that contribute to η' meson production in pp collisions. Their contributions can be estimated in a systematic way following Ref. [18] and are found to be negligible.

IV. NUMERICAL RESULTS AND DISCUSSION

Once all the ingredients are specified, the total cross section for the reaction $p + p \rightarrow p + p + \eta'$ can be calculated. We will first analyze each current separately, exploring the role of individual contributions and the uncertainties associated with them, and then combine them later in the section.

The N^* resonance current contribution to the total cross section as a function of excess energy Q is shown in Fig. 2. The excess energy is defined as $Q \equiv \sqrt{s} - \sqrt{s_o}$, where \sqrt{s} denotes the total center-of-mass energy of the system and $\sqrt{s_o} \equiv 2m_N + m_{\eta'}$, its η' -production threshold energy. Here we also display the recent experimental data from the COSY-11 [6] and SPESIII [7] collaborations. The mixing parameter λ in Eq.(10) for the $NN^*\pi$ vertices is fixed to be $\lambda = 0$. Hereafter N^* stands for both the $S_{11}(1897)$ and $P_{11}(1986)$ resonances unless otherwise indicated. The upper panel shows the results with $\lambda = 0$ in the $NN^*\eta'$ vertices. We see that the cross section is largely dominated by the $S_{11}(1897)$ contribution (dash-dotted line). The $P_{11}(1986)$ resonance leads to an energy dependence (dashed line) of the cross section steeper than that of the $S_{11}(1897)$ resonance, although in the excess energy region considered its contribution is practically negligible. The solid line corresponds to the total contribution, which is close to the data. The lower panel corresponds to the choice of $\lambda = 1$ at the $NN^*\eta'$ vertices. Compared to the case of $\lambda = 0$, we see that the mixing parameter has practically no influence on the $S_{11}(1897)$ contribution. This is due to the fact that this resonance is practically on its mass shell in the near-threshold energy region, so that both choices of the parameter λ are equivalent. Although still very small compared to the $S_{11}(1897)$ contribution, the $P_{11}(1986)$ resonance contribution increases substantially in the low excess energy region compared to the $\lambda = 0$ case. This is because this resonance is off-shell and the ps coupling mixes efficiently the positive and negative energy states. The pv coupling ($\lambda = 0$) suppresses this mixing. The interference with the $S_{11}(1897)$ contribution is now destructive. In this case the total contribution (solid curve) is slightly reduced compared to that in the upper panel. These results are consistent with the recent analysis of η' photoproduction [16]. We recall that the coupling constants at the $NN^*\eta'$ and $NN^*\pi$ vertices entering in the resonance current have been determined from the decay widths extracted in Ref. [16].

Although we find the consistency between our result above for $pp \rightarrow pp\eta'$ and the η' photoproduction analysis of Ref. [16], care must be taken in drawing any premature conclusions about the basic η' production mechanisms in these reactions. As mentioned in

subsection III.B, given the assumptions made in Ref. [16] in the extraction of the partial decay widths, the corresponding coupling constants, $g_{NN^*\eta'}$ and $g_{NN^*\pi}$, are subject to considerable uncertainties. In particular, the resonance dominance assumption does not allow any other possible production mechanism. As we shall show below, the vector-meson exchange current yields also a cross section comparable to the data. This indicates that the resonance current contribution shown in Fig.1 is probably overestimated. Another source of uncertainty in the resonance current arises from the off-shell form factors introduced at the $NN^*\pi$ vertex. Although the dominant $S_{11}(1897)$ resonance contribution is insensitive to the form factor at the $NN\eta'$ vertex because the resonance is nearly on its mass shell near the threshold energy, the corresponding exchanged pion (see Fig.1) is far off-shell. This makes the resonance contribution very sensitive to the form factor involving this pion. In the present calculation we have employed the same monopole form factor used at the $NN\pi$ vertex entering in the NN potential V in Eq.(2) with the cutoff parameter of $\Lambda_\pi = 0.8 \text{ GeV}$. One might then argue that, within the resonance dominance assumption, the $\gamma p \rightarrow p\eta'$ and $pp \rightarrow pp\eta'$ processes can be described consistently—provided that one uses a soft form factor at the $NN^*\pi$ vertex. Whatever the arguments, it is clear that further investigation is required in order to determine better the relevant coupling constants before a more definite conclusion can be drawn about the role of the nucleon resonance current in the $pp \rightarrow pp\eta'$ reaction. Of course one should also keep in mind the possibility that the strong peak in the cross section observed in η' photo-production close to threshold may be due to a cusp effect [29] and *not* due to a resonance.

We turn now to investigate the mesonic current contribution, which is displayed in Fig. 3. Among the exchange currents considered, the $\rho\rho\eta'$ exchange gives rise to the dominant contribution (dashed line). The $\omega\omega\eta'$ - and $\sigma\eta\eta'$ -exchange current contributions (dotted and dash-dotted line, respectively) are of similar magnitude. However they are smaller by about a factor of five compared to the $\rho\rho\eta'$ -exchange contribution. The slightly different energy dependence of the cross section resulting from the $\rho\rho\eta'$ - and $\omega\omega\eta'$ -exchange currents is due to the tensor coupling in the $NN\rho$ vertex. This coupling is absent in the $NN\omega$ vertex

used here. As mentioned in subsection III.C, the sign of the $\sigma\eta\eta'$ -exchange current relative to $vv\eta'$ -exchange currents ($v = \rho, \omega$) is not fixed; therefore we consider both possibilities. Assuming the negative sign for $g_{\sigma\eta\eta'}$, the interference with the $vv\eta'$ -exchange current is destructive, yielding the total contribution represented by the solid line. If $g_{\sigma\eta\eta'}$ is positive, then the interference is constructive and gives the total contribution shown by the dotted line. Although this latter choice leads to an overprediction of the data, we cannot exclude it at this stage because, as we shall show below, the nucleonic current can interfere destructively with the mesonic current so that the combined contribution may be smaller than that of mesonic current alone. Moreover, the off-shell form factor at the η' -production vertices in the mesonic current is not well-determined at present. As mentioned in subsection III.C, we employ the same form factors at the $\pi\rho\omega$ and $\pi\rho\phi$ vertices as in the study of ω - and ϕ -meson production in pp collisions [18], which are themselves subject to considerable uncertainties. Indeed, a reduction of about 10% in the value of the cutoff parameter can bring the short-dashed curve in Fig. 3 onto the data. Therefore neither sign of $g_{\sigma\eta\eta'}$ can be excluded from the present analysis. In this regard, measurements of cross sections at higher excess energies may be useful in deciding between the two choices of the sign in the $\sigma\eta\eta'$ coupling.

In the upper panel of Fig. 4, the nucleonic current contribution (dashed curve) is shown with pv coupling at the $NN\eta'$ vertex. The contribution from the mesonic current with the choice of positive sign for $g_{\sigma\eta\eta'}$ (dashed curve in Fig. 3) is also shown here as the dash-dotted curve. As we can see, the nucleonic current is about two orders of magnitude smaller than the mesonic current. Their interference is constructive and results in the total contribution shown by the solid curve, which overpredicts the data. The lower panel of Fig. 4 shows the same results, except that ps coupling is used at the $NN\eta'$ vertex in the nucleonic current contribution. Compared to the case of pv coupling, we observe a considerable enhancement of the nucleonic current. This is due to the strong admixture of the positive and negative energy nucleon states provided by the ps coupling; with pv coupling this mixing is suppressed. Furthermore the interference with the mesonic current is now destructive, resulting in a total contribution (solid line) that is substantially smaller than the mesonic current contribution

alone. Fig. 5 shows the same results as in Fig. 4, except that here the mesonic current contribution corresponds to the choice of negative sign for $g_{\sigma\eta\eta'}$ (solid curve in Fig. 3). We see a similar feature to that observed in Fig. 4, yielding net cross sections that underpredict the data. In particular, we see a strong destructive interference between the mesonic and nucleonic currents in the case of the ps coupling at the $NN\eta'$ vertex (lower panel). We observe that the effect of the nucleonic current may be overestimated here because we have used a rather large $NN\eta'$ coupling constant, as discussed in subsection III.A. In any case, given the fact that the nucleonic current is small compared to other currents, a quantitative determination of the $NN\eta'$ coupling constant using the $pp \rightarrow pp\eta'$ reaction is unlikely to be possible—at least not before the other dominant currents are better understood.

The above considerations expose the role of individual currents as well as the current uncertainties associated with them in the description of the $pp \rightarrow pp\eta'$ reaction. We combine now all the currents. In the following we consider all the possibilities for the mesonic-plus-nucleonic current contribution as shown in Figs. 4 and 5. For each scenario considered we adjust the coupling constants $g_{NN^*\eta'}$ and $g_{NN^*\pi}$ in the resonance current so as to reproduce the data, taking $\lambda = 1$ in the $NN^*\eta'$ vertices. The results are shown in Fig. 6. For the case of the mesonic-plus-nucleonic current shown in the upper panel of Fig. 4, the corresponding resonance contribution is set to zero because the mesonic-plus-nucleonic current already overpredicts the data and the resonance current can only enhance the cross section further. We recall that the interference between the resonance and other currents is practically negligible. Therefore we have here adjusted the ps-pv mixing parameter in the $NN\eta'$ vertex to $\lambda = 0.7$ in order to reproduce the data, and the corresponding result is shown in the solid curve of Fig. 6. For the choice of the mesonic-plus-nucleonic current as shown in the lower panel of Fig. 4, the resonance current is required in order to reproduce the data. We have adjusted this current contribution by multiplying the product of the coupling constants $g_{NN^*\eta'}g_{NN^*\pi}$ for both $N^* = S_{11}(1897)$ and $P_{11}(1986)$ resonances by an arbitrary reduction factor of $1/2$. The result is shown by the dash-dotted line. For the scenario of the mesonic-plus-nucleonic current shown in the upper panel of Fig. 5, the reduction factor

of the product $g_{NN^*\eta'}g_{NN^*\pi}$ required in the resonance current is 0.625. The corresponding result is shown by the dotted curve. Finally, for the scenario of the lower panel in Fig. 5, no reduction of the resonance current is required in order to reproduce the data, since this corresponds to an extreme case where the destructive interference between the nucleonic and mesonic currents leads to a mesonic-plus-nucleonic current contribution that is nearly negligible. The short-dashed curve is the corresponding result. Fig. 6 reveals the different energy dependences arising from each scenario considered. We see that if one wants to learn about the production mechanism from the total cross section then one has to go to much higher energy region than that covered by the presently available data.

At this point we note that, in view of the latter scenario discussed in Fig.6 above, it is not surprising that the approach of Ref. [8] describes the $pp \rightarrow pp\eta'$ data. In Ref. [8] the $\pi N \rightarrow \eta' N$ amplitude, extracted from the measured cross section, has been used as the production mechanism. The $\pi N \rightarrow \eta' N$ amplitude obtained in this way must include the nucleon resonance contribution that we have considered in this work, which leads to a strong $\pi N \rightarrow \eta' N$ transtion. We emphasize, however, that one has to be careful in drawing any premature conclusion here. First, as discussed before, our nucleon resonance current is subject to considerable uncertainties. Second, although the calculation of Ref. [8] is based on the measured $\pi N \rightarrow N\eta'$ cross section, it requires an introduction of an off-shell form factor at the $NN\pi$ vertex in order to account for the off-shellness of the exchanged pion. As we have pointed out, the exchanged pion is far off-shell in the present reaction and consequently the resulting cross sections are very sensitive to the corresponding form factor at the $NN\pi$ vertex. We note that in Ref. [8] a monopole form factor with the cutoff parameter of $\Lambda_\pi = 1.3 \text{ GeV}$, as used in the Bonn NN potential, has been employed. There are, however, a number of indications that the $NN\pi$ form factor is much softer ($\Lambda_\pi \sim 0.8 \text{ GeV}$) than that used in the Bonn potential [35,36]. This would reduced the contribution of the one-pion exchange to the $pp \rightarrow pp\eta'$ process substantially. The above consideration gives an idea of the kind of uncertanties involved in the theoretical predictions.

We now focus our attention on the excess energy region close to threshold where the data

exist. Fig. 7 shows the results of Fig. 6 in the range of excess energy up to $Q = 10 \text{ MeV}$. Here, only one total current contribution (solid curve in Fig. 6) is shown since all four scenarios considered lead to almost indistinguishable results at the scale used in the limited energy domain considered in the figure. We note that the energy dependence of the cross section is not reproduced. In particular, after adjusting the ps-pv mixing parameter or the reduction factor of $g_{NN^*\eta'}g_{NN^*\pi}$ in order to reproduce the higher energy data points, as has been done in Fig. 6, we are not able to describe the lowest two data points. We observe that the data have considerable uncertainties in the excess energy, presumably due to background subtraction that becomes more difficult for energies very close to the threshold. Nevertheless the results indicate the need for some mechanism(s) that introduces an additional energy dependence of the total cross section very close to threshold. The energy dependence of the total cross section near threshold is basically determined by the final state NN interaction [12]. This is illustrated by the dotted line in Fig. 7, which corresponds to the result calculated taking into account only the three-body phase space-plus-final state interaction; it has been normalized to the solid curve in the low excess energy region. We see that the production currents start to modify the energy dependence given by the phase space-plus-final state interaction only for energies above $Q = 4 - 5 \text{ MeV}$. Therefore the predicted energy dependence in the near- threshold region is unlikely to be modified by the *basic* production mechanism(s). In fact, all the individual currents considered in this work lead practically to the same energy dependence in the restricted energy range considered in Fig. 7.

The fact that the energy dependence given by the three-body phase space-plus-final state interaction does not reproduce the observed energy dependence in $pp \rightarrow pp\eta'$ process has been a subject of attention since the publication of the COSY-11 data [6,9,11]. In Fig. 8 we show the measured cross section data for π^0 , η and η' production in pp collisions together with the corresponding energy dependence predicted by the phase space-plus-final state interaction only (solid curves). Apart from the fact that in η' production the deviation starts a little lower in excess energy than in π^0 production, we see no indication for any peculiar feature in η' production.

The most trivial source of influence on the energy dependence of the cross section close to threshold is the Coulomb force [13], which has not been considered so far in our calculations. We follow the Gell-Mann and Goldberger two-potential formalism [37] to include the Coulomb force in the final state interaction. The perturbed wave function is calculated exactly by solving the Schrödinger equation in coordinate space with the nuclear-plus-Coulomb potential. For the nuclear potential we use the Paris potential [38]. The half-off-shell (pure) Coulomb T-matrix is obtained in analytic form [39]. We note that care must be taken in order to use consistently a NN T-matrix constructed within a non-relativistic formulation—such as the Paris T-matrix—in a relativistic approach. We have followed Ref. [40] in order to use the Paris T-matrix in the present relativistic approach. Also, in the following, the production current has been kept the same as that used in conjunction with the Bonn B potential, except for a readjustment of the reduction factor of the product $g_{NN^*\eta'}g_{NN^*\pi}$ in the nucleon resonance current that was needed to reproduce the data. We are aware that by using the Paris potential instead of the Bonn B potential we may lose the consistency between the production current and the final state interaction, however the energy dependence of the cross section is practically the same—when the Coulomb force is switched off—as that given by the Bonn B potential over a wide range of excess energy. The result of including the Coulomb effect as described above is shown in Fig. 9 by the solid line. The dotted line corresponds to the result when the Coulomb force is switched off. As can be seen, the Coulomb effect is considerable; in particular, it reduces the cross section by almost 40% at $Q = 1.5 \text{ MeV}$.

The picture that emerges from the above considerations is that there is no obvious indication of a need for other mechanisms than those already considered here in order adequately to describe the existing data. A close comparison of the COSY-11 [6] and SPESIII [7] data, however, seems to indicate different trends in the energy dependence. In this connection, new measurements at higher energies, and even remeasurement of some of the data near $Q \sim 4 \text{ MeV}$, are extremely important for resolution of this issue. The new data at higher energies will certainly impose more stringent constraints on the parameters of our model.

They would also tell us whether a proper description of the $pp \rightarrow pp\eta'$ requires the inclusion of the $p\eta'$ final state interaction, as has been argued recently [11]. The $p\eta'$ final state interaction as discussed in Ref. [11] can be viewed as the higher order terms in the production current treated in the present work. In fact, the η' -emission current defined in the previous section (cf. Eqs.(5,8,21)) is, in part, just the Born term of a more general current that can be obtained by using the T-matrix amplitude for the $M + p \rightarrow \eta' + p$ transition, where M denotes any meson of interest. This can easily be seen if we disregard the nucleon labeled 2 in Fig. 1; the current then becomes nothing other than the Born term of the $M + p \rightarrow \eta' + p$ transition amplitude. The T-matrix amplitude for the $M + p \rightarrow \eta' + p$ process may be separated into the so-called pole and non-pole terms according to Pearce and Afnan [41]. By using the physical baryon mass and physical $NB\eta'$ ($B = N, N^*$) and NNM vertices in the baryonic current, the pole term of the $M + p \rightarrow \eta' + p$ T-matrix amplitude is fully accounted for in the present work. What is taken in the Born approximation is, therefore, the non-pole part of the T-matrix only.

V. SUMMARY

We have investigated the reaction $pp \rightarrow pp\eta'$ within a relativistic meson-exchange model of hadronic interactions. We find that the $S_{11}(1897)$ resonance as determined in a recent multipole analysis of η' photoproduction [16] gives rise to a contribution that reproduces the measured cross section and allows for no other production mechanisms. This is consistent with the analysis of Ref. [16], where the nucleon resonance parameters have been extracted under the resonance dominance assumption. Whether this is already the entire physics of the production mechanism is an open question that requires further investigation. Indeed, in Ref. [16], in addition to the assumption of resonance dominance, only the $p\eta'$ and $p\pi^0$ decay channels have been explicitly considered; the $p\pi^0$ decay channel accounts for *all* possible decay channels other than the $p\eta'$. The coupling constants $NN^*\eta'$ and $NN^*\pi$ obtained from the decay widths extracted under these assumptions are, therefore, subject to considerable

uncertainties which, in turn, lead to corresponding uncertainties in the resonance current contribution to the cross section. A more accurate determination of the relevant resonance parameters is called for before a more definite conclusion can be drawn about the role of the N^* resonances in the $pp \rightarrow pp\eta'$ reaction. We should also keep in mind that the strong peak in the cross section close to threshold in η' photoproduction may be due to a cusp effect [29], and not to the resonance assumed in Ref. [16]. All these issues associated with the resonance require further careful investigation.

The mesonic current gives rise to cross sections which are comparable to the measured values. It is dominated by the $\rho\eta'$ -exchange current. Depending on the choice of the sign of the $\sigma\eta\eta'$ coupling constant, the calculated cross sections overpredict or underpredict the data. However neither choice can be excluded at present—mainly due to uncertainties associated with the baryonic current. Data in higher energy regions than currently available may provide the necessary constraint to fix the sign of this coupling, as the different signs lead to different energy dependences.

Since the nucleonic current is found to be small, it is unlikely that the $pp \rightarrow pp\eta'$ reaction can be used quantitatively to determine the $NN\eta'$ coupling constant—at least not before the other dominant currents are under better control.

As expected from earlier calculations [13], the Coulomb force in the final state interaction is found to play a crucial role in explaining the observed energy dependence of the cross section close to threshold. The basic production mechanisms start to influence the energy dependence of the cross section only for excess energies above ~ 5 MeV. For lower energies the energy dependence is determined by the three-body phase space-plus-final state interaction [12]. New data at higher energies will certainly impose constraints on the production mechanisms. In addition to more exclusive observables than the total cross section, a combined analysis of production processes using both electromagnetic and hadronic probes should help to disentangle the different production mechanisms.

Acknowledgment We are grateful to J. Haidenbauer and S. Krewald for useful discussions. We also thank Ulf Meißner and J. Haidenbauer for critical readings of the manuscript.

H.F.A. acknowledges the partial support from FONDECYT, grant No. 1970508.

REFERENCES

- [1] B. Diekmann, Phys. Rep. **159**, 99 (1988); J. Jousset et al., Phys. Rev. **D41**, 1389 (1990); P. Ball, J.-M. Frere and M. Tygat, Phys. Lett. **B365**, 367 (1996).
- [2] CLEO Collaboration, B. H. Behrens et al., Phys. Rev. Lett. **80**, 3710 (1998); T. E. Browder et al., Phys. Rev. Lett. **81**, 1786 (1998).
- [3] D. Atwood and A. Soni, Phys. Lett. **B405**, 150 (1997); Phys. Rev. Lett. **79**, 5206 (1997); W-S. Hou and B. Tseng, Phys. Rev. Lett. **80**, 434 (1998); M. R. Ahmady, E. Kou, and A. Sugamoto, Phys. Rev. **D58**, 14014 (1998); For a most recent determination of the η' gluonic admixture, see E. Kou, hep-ph/9908214.
- [4] J. Ashman et al., Phys. Lett. **B206**, 364 (1988).
- [5] A. V. Efremov, J. Soffer, and N. A. Törnqvist, Phys. Rev. Lett. **64**, 1495 (1990); Phys. Rev. **D44**, 1369 (1991); S. Narison, G. M. Shore, and G. Veneziano, Nucl. Phys. **B546**, 235 (1999) and references therein.
- [6] P. Moskal et al., Phys. Rev. Lett. **80**, 3202 (1998).
- [7] F. Hibou et al., Phys. Lett. **B438**, 41 (1998).
- [8] A. Sibirtsev and W. Cassing, Eur. Phys. J. **A2**, 333 (1998).
- [9] V. Bernard, N. Kaiser and U. Meißner, Eur. Phys. J. **A4**, 259 (1999).
- [10] E. Gedalin, A. Moalem and L. Razdolskaja, Nucl. Phys. **A650**, 471 (1999).
- [11] V. Baru, J. Haidenbauer, C. Hanhart, A. Kudryavtsev and J. Speth, Eur. Phys. J. **A.**, in press.
- [12] K. Watson, Phys. Rev. **88**, 1163 (1952). For a recent discussion, see Ref. [15].
- [13] G. A. Miller and P. U. Sauer, Phys. Rev. **C44**, R1725 (1991).
- [14] V. Herrmann, K. Nakayama, H. F. Arellano, and O. Scholten, Nucl. Phys. **A582**, 568

- (1995).
- [15] C. Hanhart and K. Nakayama, Phys. Lett. **B454**, 176 (1999).
 - [16] R. Plötzke et al., Phys. Lett. **B444**, 555 (1998).
 - [17] K. Nakayama, A. Szczurek, C. Hanhart, J. Haidenbauer and J. Speth Phys. Rev. **C57**, 1580 (1998).
 - [18] K. Nakayama, J.W. Durso, J. Haidenbauer, C. Hanhart and J. Speth, Phys. Rev. **C**, in press; nucl-th/9904040.
 - [19] J. Haidenbauer, private communication; Following Phys. Rev. **C40**, 2465 (1989), the Bonn B potential can be constrained to the low-energy pp scattering length with only a minor readjustment of its $NN\sigma$ coupling constant in the total isospin $T = 1$ state. See also Table 1 in Ref. [14], where another version of the Bonn potential has been modified in a similar way.
 - [20] R. Machleidt, Adv. Nucl. Phys. **19**, 189 (1989).
 - [21] M. Batinic, A. Svarc and T.-S.H. Lee, *Phys.Scripta* **56**, 321 (1997).
 - [22] extracted from the VIRGINIA TECH PARTIAL-WAVE ANALYSES ON-LINE (http://said.phys.vt.edu/said_branch.html)
 - [23] O. Dumbrajs, et al. Nucl. Phys. **B216**, 277 (1983).
 - [24] J. F. Zhang, N. Mukhopadhyay and M. Benmerrouche, Phys. Rev. **C52**, 1134 (1995).
 - [25] W. Grein and P. Kroll, Nucl. Phys. **A338**, 332 (1980).
 - [26] G. Altarelli, R. D. Ball, S. Forte and G. Ridolfi, Nucl. Phys. **B496**, 337 (1997).
 - [27] S. Okubo, Phys. Lett. **5**, 165 (1963); G. Zweig, CERN Report No. TH412, 1964; J. Iizuka, Prog. Theor. Phys. Suppl. **37 & 38**, 21 (1966).
 - [28] F. E. Close and R. G. Roberts, Phys. Lett. **B316**, 165 (1993); P. G. Ratcliffe, Phys.

- Lett. **B365**, 383 (1996); X. Song, P. K. Kabir, and J. S. McCarthy, Phys. Rev. **D54**, 929 (1996).
- [29] G. Höhler, πN Newsletter **14**, 168 (1998).
- [30] M. Benmerrouche and N. C. Mukhopadhyay, Phys. Rev. **D51**, 3237 (1995).
- [31] J.W. Durso, Phys. Lett. **B184**, 348 (1987).
- [32] Particle Data Group, Eur. Phys. J. **C3**, 1 (1998).
- [33] H. Garcilazo and E. Moya de Guerra, Nucl. Phys. **A562**, 521 (1993).
- [34] C. Schütz, J. W. Durso, K. Holinde and J. Speth, Phys. Rev. **C49**, 2671 (1994).
- [35] K. F. Liu, S. J. Dong, T. Draper, and W. Wilcox, Phys. Rev. Lett. **74**, 2172 (1995).
- [36] R. Bockmann, C. Hanhart, O. Krehl, S. Krewald, and J. Speth, Phys. Rev. **C**, in press; nucl-th/9905043.
- [37] M. Gell-Mann and M. L. Goldberger, Phys. Rev. **91**, 398 (1953).
- [38] M. Lacombe, B. Loiseau, J. M. Richard, R. Vinh Mau, J. Côté, P. Pirès and R. de Tournreil, Phys. Rev. **C21**, 861 (1980).
- [39] Dilinskii and Mukhamedzhanov, Soviet J. Nucl. Phys. **3**, 180 (1966).
- [40] V. Herrmann and K. Nakayama, Phys. Rev. **C46**, 2199 (1992).
- [41] B. C. Pearce and I. R. Afnan, Phys. Rev. **C34**, 991 (1986).
- [42] H. O. Meyer et al., Phys. Rev. Lett. **65**, 2846 (1990). Corrected data according to Ref. [43].
- [43] H. O. Meyer et al., Nucl. Phys. **A539**, 633 (1992).
- [44] A. Bondar et al., Phys. Lett. **B356**, 8 (1995).
- [45] E. Chiavassa et al., Phys. Lett. **B322**, 270 (1994).

[46] H. Calén et al., Phys. Lett. **B366**, 39 (1996).

FIGURES

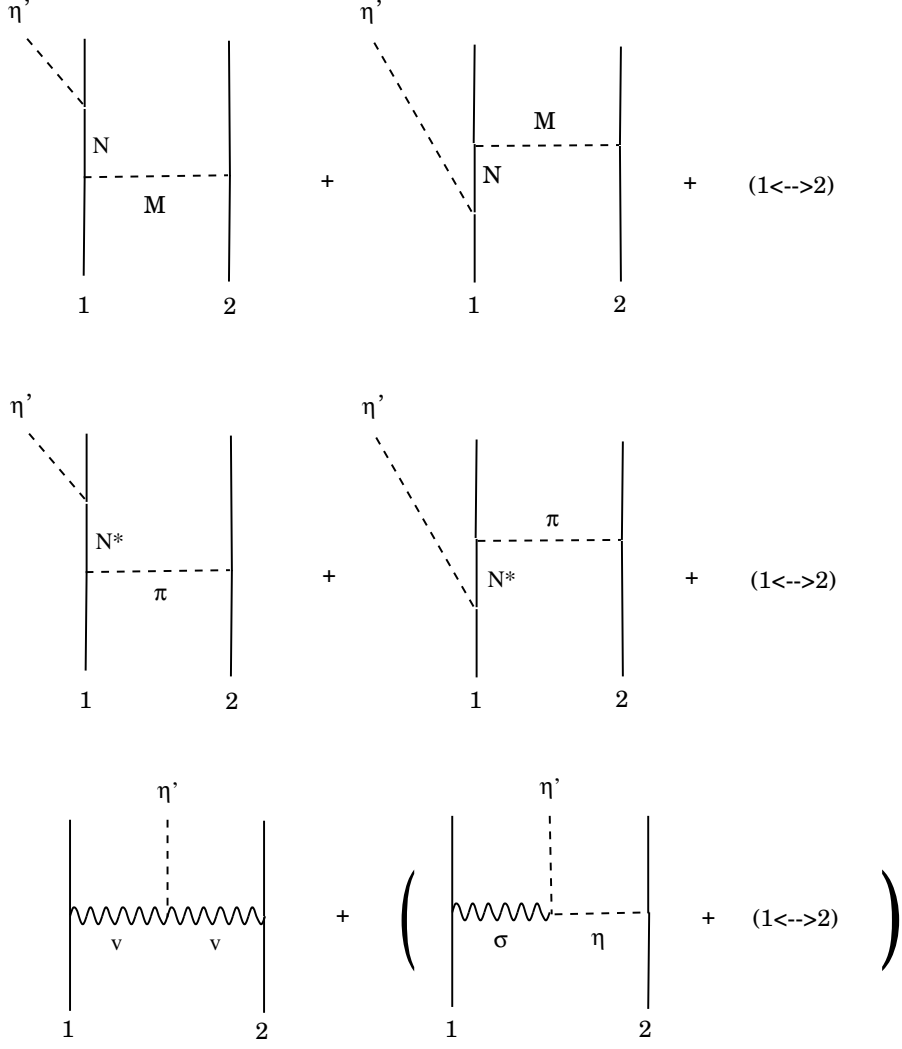


FIG. 1. η' meson production currents included in the present study. Upper row: nucleonic current J_{nuc} , $M = \pi, \eta, \rho, \omega, \sigma, a_0$. Middle row: nucleon resonance current J_{res} , $N^* = S_{11}(1897), P_{11}(1986)$. Lower row: mesonic current J_{mes} , $v = \rho, \omega$.

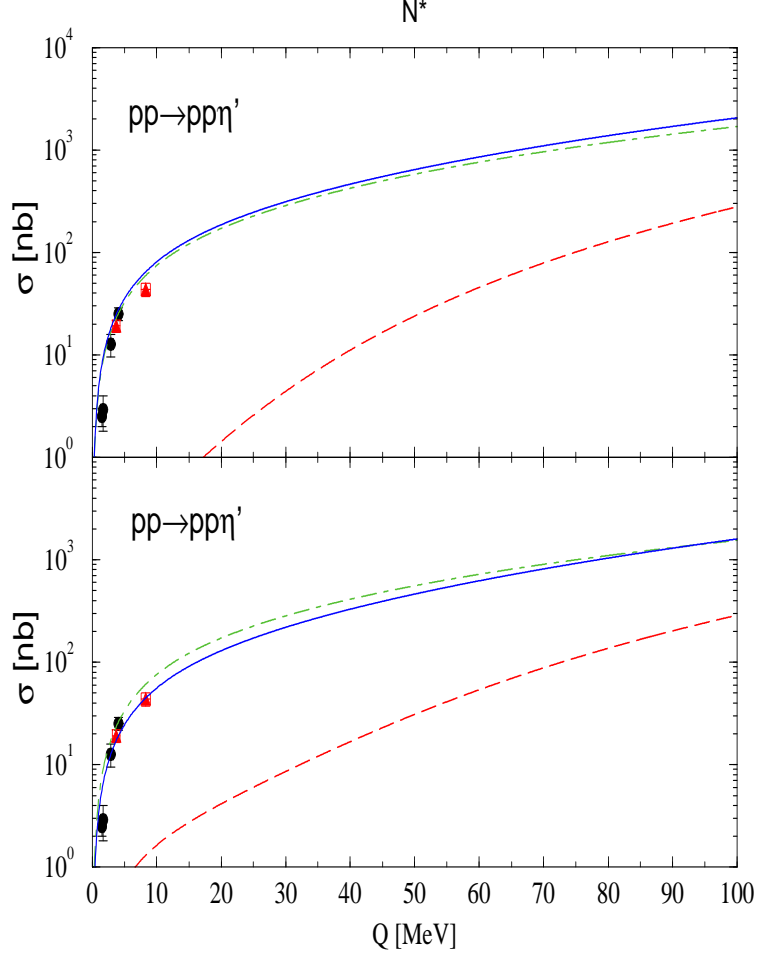


FIG. 2. N^* resonance current contribution to the total cross section for the reaction $pp \rightarrow pp\eta'$ as a function of excess energy Q . The upper panel corresponds to the results with the choice $\lambda = 0$ in Eq.(10) at the $NN^*\eta'$ vertices, the lower panel to those with the choice $\lambda = 1$. The dashed-dotted curves correspond to the $S_{11}(1897)$ resonance contribution, the dashed curves to the $P_{11}(1986)$ resonance contribution. The solid curves are the total contributions. The experimental data are from Refs. [6,7].

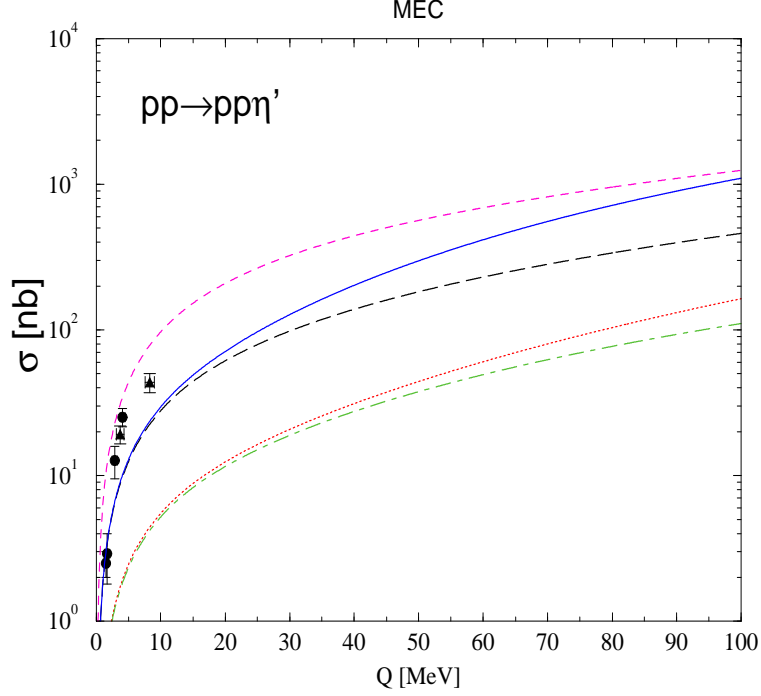


FIG. 3. Mesonic current contribution to the total cross section for the reaction $pp \rightarrow pp\eta'$ as a function of excess energy Q . The dash-dotted curve correspond to the $\sigma\eta\eta'$ -exchange and the dotted curve to the $\omega\omega\eta'$ -exchange current contribution. The dashed curve represents the $\rho\eta'$ -exchange current contribution. The solid curve is the total contribution corresponding to choosing the negative sign for the $\sigma\eta\eta'$ coupling constant, the short-dashed curve to the positive sign. The experimental data are from Refs. [6,7].

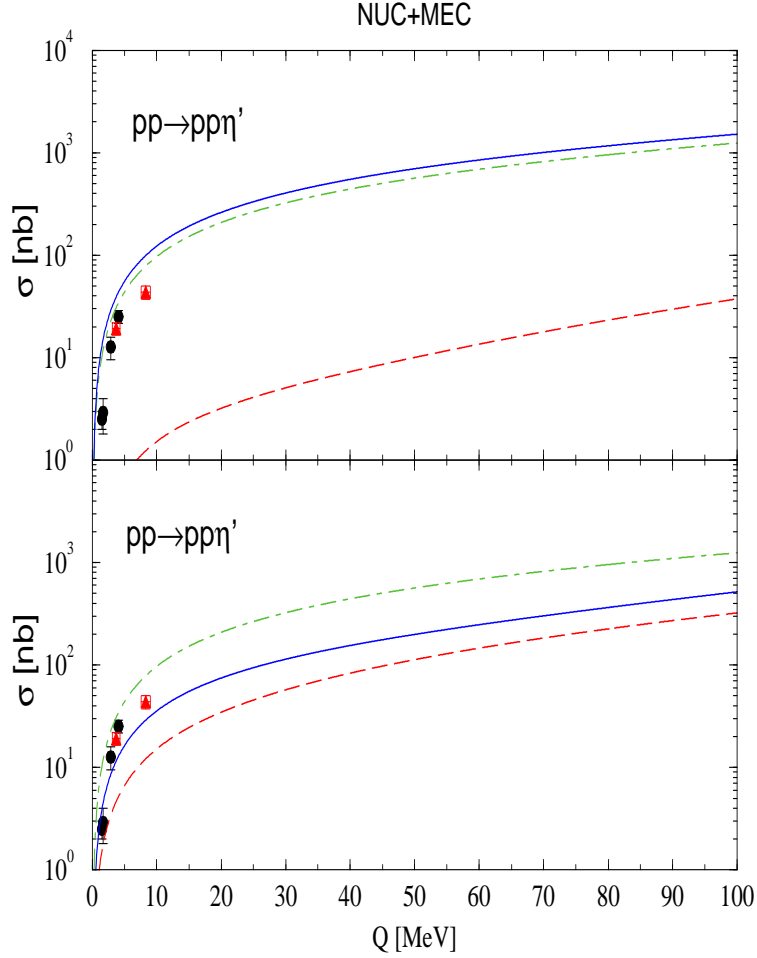


FIG. 4. Nucleonic-plus-mesonic current contributions to the total cross section for the reaction $pp \rightarrow pp\eta'$ as a function of excess energy Q . The upper panel corresponds to the results with the pv coupling ($\lambda = 0$) at the $NN'\eta'$ vertex in the nucleonic current, the lower panel to those with ps coupling ($\lambda = 1$). The dashed-dotted curve in both panels represents the total mesonic current contribution shown by the dashed curve in Fig. 3. The nucleonic current contributions are represented by the dashed curves and the corresponding total contributions by the solid curves. The experimental data are from Refs. [6,7].

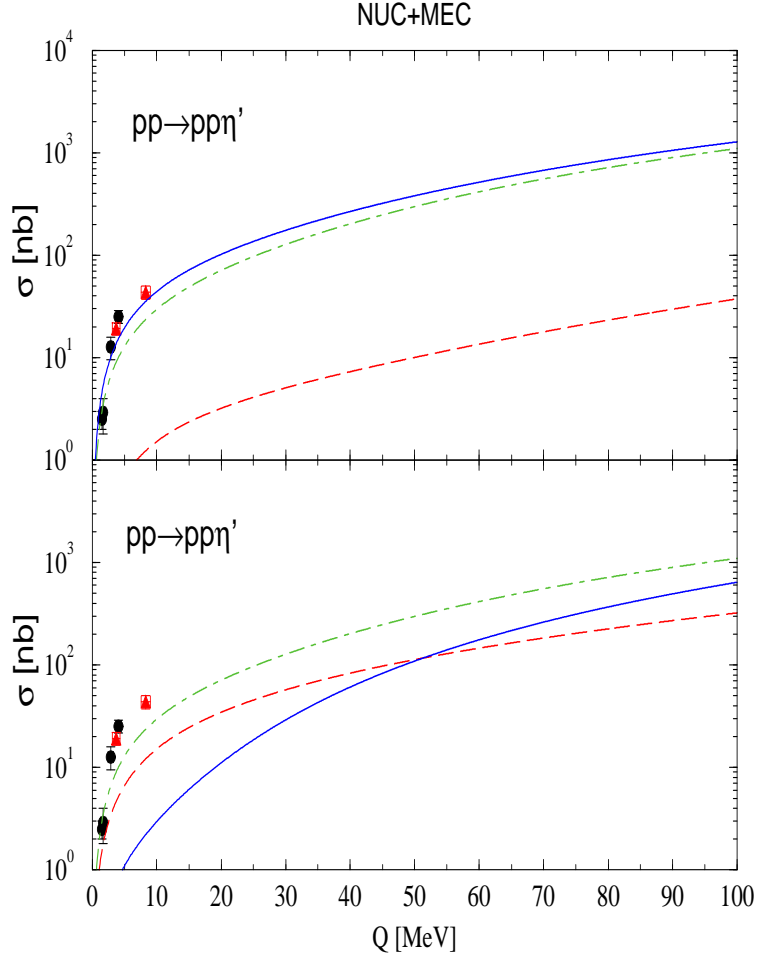


FIG. 5. Same as Fig. 4, except for the total mesonic current contribution, which corresponds to the result represented by the solid curve in Fig. 3

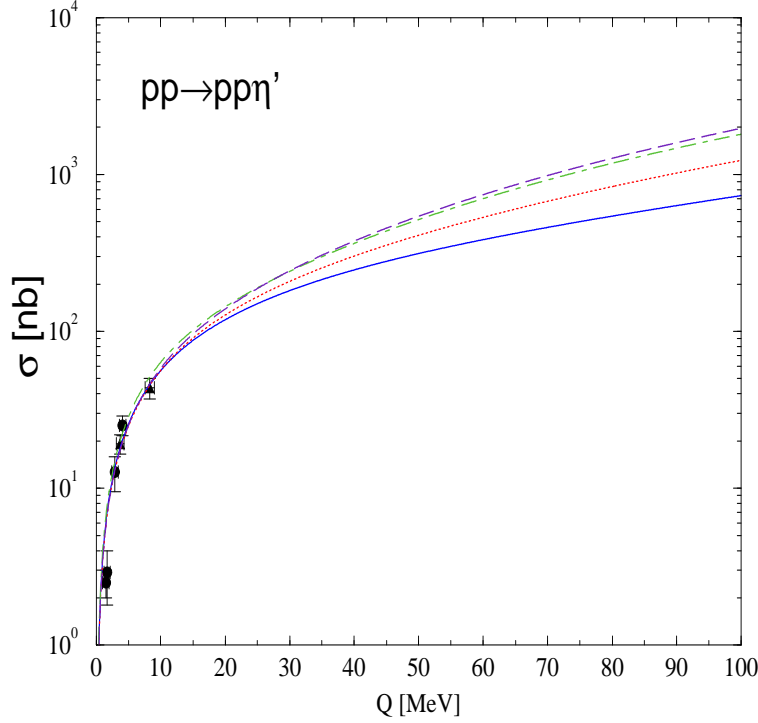


FIG. 6. The total cross section for the reaction $pp \rightarrow pp\eta'$ as a function of excess energy Q . The solid line represents the mesonic-plus-nucleonic current contribution corresponding to the upper panel of Fig. 4, except for the value of the ps-pv mixing parameter at the $NN\eta'$ vertex, which is taken to be $\lambda = 0.7$. The dotted line represents the result corresponding to the mesonic-plus-nucleonic current shown in the lower panel of Fig. 4; it includes also the nucleon resonance current, whose product of the coupling constants $g_{NN^*\eta'}g_{NN^*\pi}$ is multiplied by an arbitrary reduction factor of $1/2$. The dash-dotted and dashed curves are the same as the dotted curve, except that they correspond to the mesonic-plus-nucleonic current shown in the upper and lower panels of Fig. 5, respectively. The corresponding reduction factors of the product $g_{NN^*\eta'}g_{NN^*\pi}$ are 0.625 and 1. The experimental data are from Refs. [6,7].

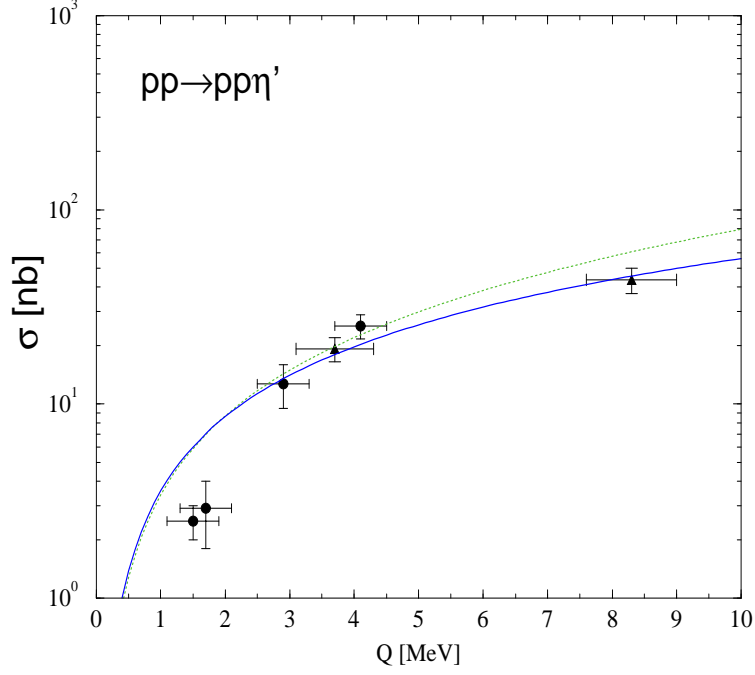


FIG. 7. Same as Fig. 6 for excess energy below 10 MeV . Only one total contribution (solid curve) is shown since all the curves shown in Fig. 6 are almost indistinguishable at the scale used here. The dotted line corresponds to the result with only the phase space-plus-final state interaction.

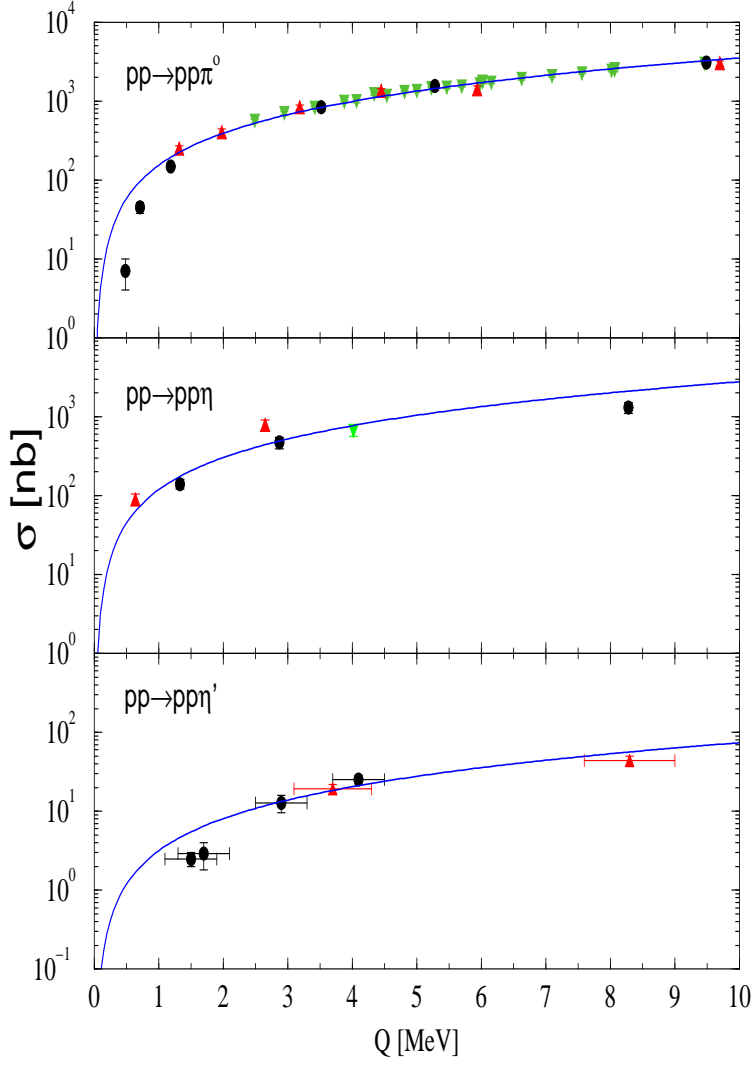


FIG. 8. The total cross section for π^0 -, η - and η' -meson production in pp collisions as a function of excess energy Q . The curves represent the corresponding energy dependence given by the phase space-plus-final state interaction with *no* Coulomb force. In the upper panel the experimental data are from Refs. [42–44]; in the middle panel from Refs. [7,45,46]; in the lower panel from Refs. [6,7].

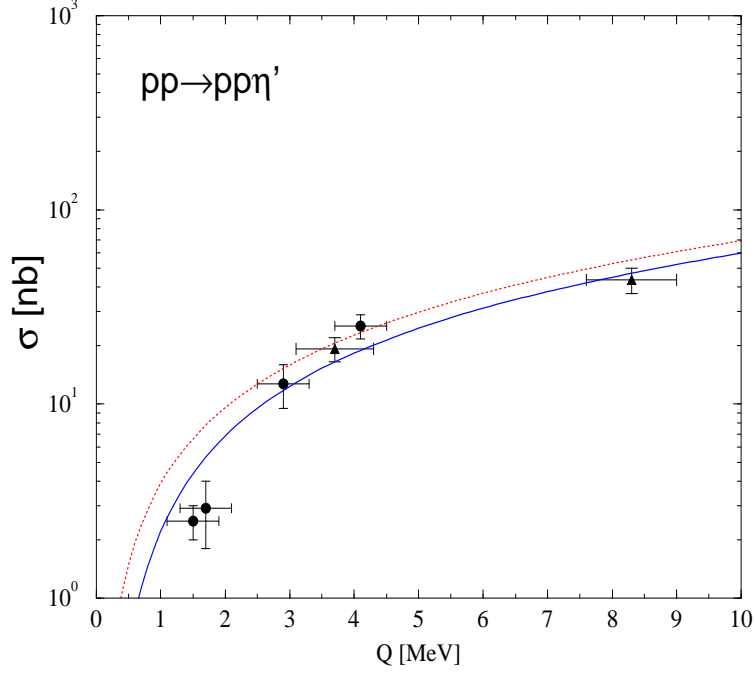


FIG. 9. The total cross section for the reaction $pp \rightarrow pp\eta'$ as a function of excess energy Q . The solid curve corresponds to the total current contribution including the Coulomb force in the final state interaction. The dotted line corresponds to that when the Coulomb force is switched off. Here the Paris T-matrix has been used as the final state interaction. The experimental data are from Refs. [6] (circle) and [7] (triangle).